

Supplement of Atmos. Chem. Phys., 16, 10671–10687, 2016
<http://www.atmos-chem-phys.net/16/10671/2016/>
doi:10.5194/acp-16-10671-2016-supplement
© Author(s) 2016. CC Attribution 3.0 License.



Atmospheric
Chemistry
and Physics
Open Access
EGU

Supplement of

Chemical characteristics and causes of airborne particulate pollution in warm seasons in Wuhan, central China

Xiaopu Lyu et al.

Correspondence to: Hai Guo (ceguohai@polyu.edu.hk)

The copyright of individual parts of the supplement might differ from the CC-BY 3.0 licence.

Section 1 Explanation of higher EC apportioned to biomass burning compared to vehicle emissions.

As a tracer of combustion, EC is generally emitted from vehicle emissions, coal combustion, biomass burning and other combustion activities. Streets et al. (2001) reviewed previous studies and estimated the emission factors of EC in China from different sectors. Results indicated that the average emission factors were 0.08 and 1.1 g/kg fuel for gasoline and diesel vehicular emissions, respectively, while they were 0.90, 0.58 and 0.72 g/kg for the field combustion of wheat, rice and corn residuals, respectively. Since diesel vehicles only accounted for 11.1% of the vehicle fleet in Wuhan (the data were available at <http://www.whepb.gov.cn/u/cms/whepb/201506/051551398i2j.pdf>), it was reasonable that more EC was apportioned to biomass burning compared to vehicular emissions.

On the other hand, May and June in summer and October and November in autumn are the periods with intensive biomass burning in and/or around Wuhan, particularly the combustion of crop residuals in agricultural provinces in central China. Namely, the intensive biomass burning during the study period was another factor leading to higher EC emitted by biomass burning than vehicular emissions.

Section 2 Explanation of the difference of coal combustion contributions between non-episode 1 and non-episode 2.

The source apportionment results indicated that contribution of coal combustion in non-episode 2 was significantly ($p < 0.05$) lower than that in non-episode 1. Bearing in mind the uncertainties caused by the lack of WSIs in summer, the lower contribution of coal combustion in non-episode 2 might be attributable to the National Day holiday from October 1 to 7. During the holiday, the coal-fired boilers in factories and power plants stopped working, which would significantly reduce PM_{2.5} emissions from coal combustion. The much lower mass contribution of coal combustion in early October (as shown in Figure S10) coincided with this inference.

Table S1 Detection limit of PM_{2.5} components.

PM _{2.5} components	Detection limit (μg/m ³)
OC	0.3
EC	0.3
SO ₄ ²⁻	0.04
NO ₃ ⁻	0.05
Cl ⁻	0.01
NH ₄ ⁺	0.05
Na ⁺	0.05
K ⁺	0.09
Mg ²⁺	0.06
Ca ²⁺	0.1
Ba	0.004
V	0.0004
Ca	0.009

Cd	0.0004
Cr	0.0011
Hg	0.004
K	0.029
Mn	0.004
Ni	0.0002
Pb	0.007
As	0.0049
Fe	0.009
Cu	0.002
Se	0.005
Zn	0.004
Ag	0.0004

Table S2 Percentage of samples with residuals between -3 and 3 (Unit: %).

PM _{2.5} components	Summer	Autumn
SO ₄ ²⁻	-	100.0
NO ₃ ⁻	-	100.0
NH ₄ ⁺	-	100.0
Cl ⁻	-	99.6
OC	97.0	99.8
EC	97.6	98.6
Ba	100.0	99.6
V	100.0	99.3
Ca	99.6	99.8
Hg	99.5	99.6
K	96.4	99.8
Mn	99.1	98.0
Ni	92.9	96.0
Pb	98.6	99.0
As	98.5	99.1
Fe	99.4	99.8
Cu	97.5	98.1
Se	97.4	99.4
PM _{2.5}	97.5	98.1

Table S3 Mass contributions to OC, SO₄²⁻, NO₃⁻ and NH₄⁺ of the resolved sources in episodes 4-6 and non-episode 2. The bold font demonstrates significant increase (increment >2 µg/m³, p<0.05) compared to non-episode 2.

	Episode 4	Episode 5	Episode 6	Non-episode 2
OC				
Fugitive dust	0.0±0.0	0.0±0.0	0.0±0.0	0.0±0.0
Oil refinery and usage	0.0±0.0	0.0±0.0	0.0±0.0	0.0±0.0
Biomass burning	12.3±0.7	5.3±0.7	4.7±0.6	5.6±0.4
Vehicle source	9.7±0.5	7.4±0.8	8.6±0.5	2.7±0.2

	Coal combustion	6.5±0.8	6.9±0.9	8.3±1.2	4.6±0.4
	SIA	0.0±0.0	0.0±0.0	0.0±0.0	0.0±0.0
SO ₄ ²⁻	Fugitive dust	1.0±0.1	0.7±0.1	0.8±0.1	0.3±0.0
	Oil refinery and usage	4.8±0.4	3.6±0.4	3.1±0.4	3.1±0.2
	Biomass burning	17.1±1.0	7.4±1.0	6.4±0.8	7.8±0.6
	Vehicle source	1.6±0.2	1.7±0.3	2.0±0.2	0.5±0.0
	Coal combustion	0.0±0.0	0.0±0.0	0.0±0.0	0.0±0.0
	SIA	5.5±0.8	9.4±1.5	10.5±1.6	4.8±0.6
NO ₃ ⁻	Fugitive dust	0.0±0.0	0.0±0.0	0.0±0.0	0.0±0.0
	Oil refinery and usage	0.0±0.0	0.0±0.0	0.0±0.0	0.0±0.0
	Biomass burning	7.0±0.4	3.0±0.4	2.6±0.3	3.2±0.2
	Vehicle source	0.0±0.0	0.0±0.0	0.0±0.0	0.0±0.0
	Coal combustion	3.6±0.5	3.9±0.5	4.6±0.6	2.6±0.2
	SIA	11.2±1.6	19.2±3.1	21.4±3.3	9.9±1.2
NH ₄ ⁺	Fugitive dust	0.2±0.01	0.1±0.02	0.1±0.01	0.0±0.0
	Oil refinery and usage	1.5±0.1	1.1±0.1	0.9±0.1	1.0±0.1
	Biomass burning	8.9±0.5	3.9±0.5	3.4±0.4	4.1±0.3
	Vehicle source	0.4±0.1	0.4±0.1	0.5±0.1	0.1±0.0
	Coal combustion	0.9±0.1	1.0±0.1	1.2±0.2	0.7±0.1
	SIA	5.5±0.8	9.3±1.5	10.4±1.6	4.8±0.6

Table S4 Speciation of SVOCs and the corresponding precursors.

Precursors	Oxidation products
Benzene	BZBIPEROOH, BZEMUCOOH, NPHENOOH
Toluene	C6H5CH2OOH, CRESOOH, NCRESOOH, TLBIPEROOH, TLEMUCOOH, C615CO2OOH
<i>m</i> -Xylene	MXYL00H, MXYBPEROOH; MXYMUCOOH
<i>o</i> -Xylene	OXYL00H, OXYBPEROOH; OXYMUCOOH
<i>p</i> -Xylene	PXYL00H, PXYBPEROOH; PXYMUCOOH
Ethylbenzene	C6H5C2OOH, C6H5C2OOH, EBENZOLOOH, NEBNZOLOOH, EBZBPEROOH, EBZMUCOOH
1,3,5-Trimethylbenzene	TMBOOH, TM135BPOOH, NTM135LOOH, TM135OLOOH, TM135MUOOH
1,2,3-Trimethylbenzene	TM123BOOH, TM123BPOOH, NTM123LOOH, TM123OLOOH, TM123MUOOH
1,2,4-Trimethylbenzene	TM124BOOH, TM124BPOOH, NTM124LOOH, TM124OLOOH, TM124MUOOH
Isoprene	NISOPOOH, ISOPAOOH, ISOPBOOH, ISOPCOOH, ISOPDOOH

2-Methyl Pentane	M2PEAOOH, M2PEBOOH, M2PECOOH, M2PEDOOH
3-Methyl Pentane	M3PEAOOH, M3PEBOOH, M3PECOOH
<i>n</i> -Hexane	HEXAOOH, HEXBOOH, HEXCOOH
<i>n</i> -Heptane	HEPTOOH
<i>n</i> -Octane	OCTOOH
<i>n</i> -Nonane	NONOOH
<i>n</i> -Decane	DECOOH
<i>n</i> -Undecane	UDECOOH

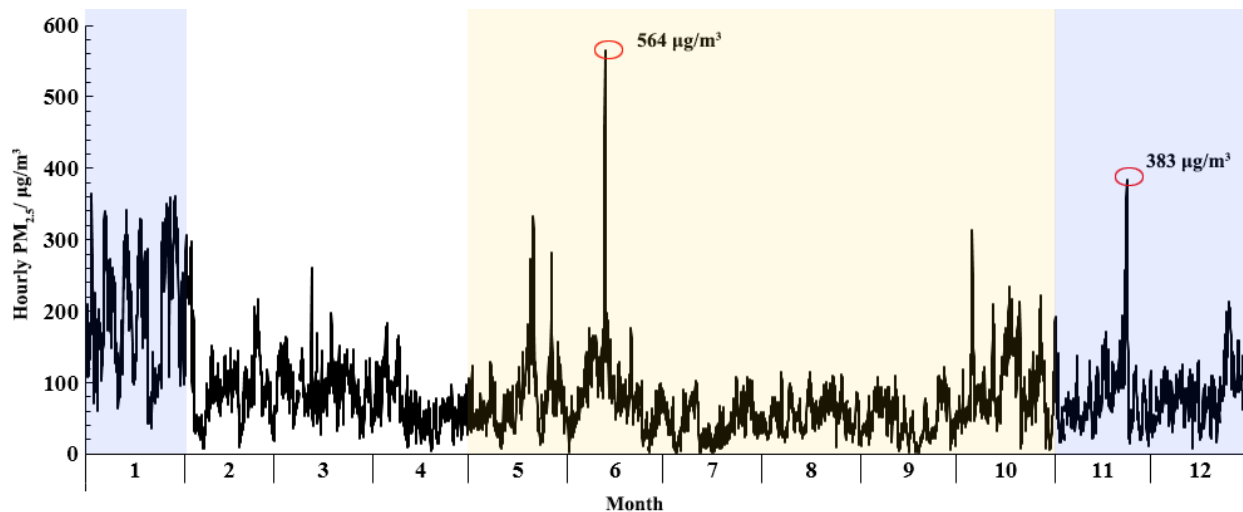


Figure S1 Hourly PM_{2.5} in Wuhan in 2014. The yellow and blue highlighted areas represent the warm seasons and winter, respectively.

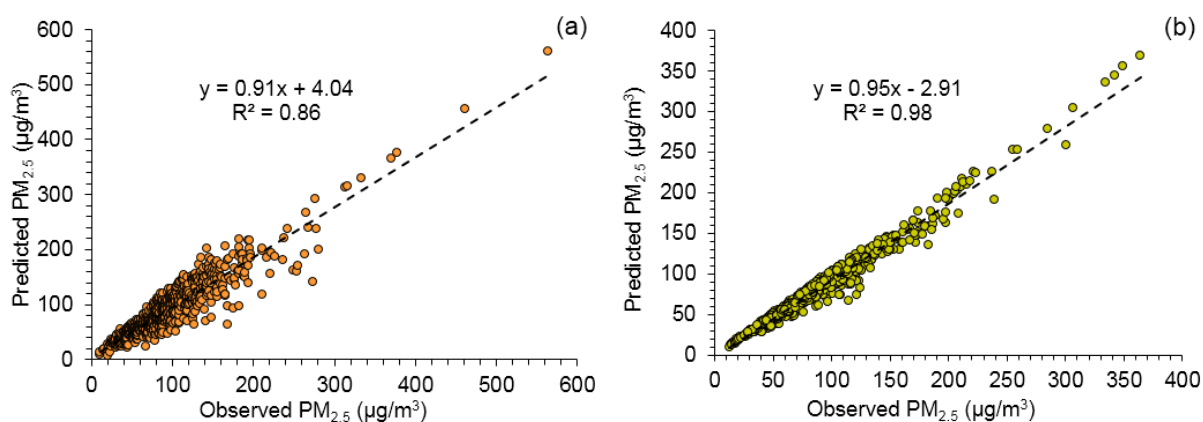


Figure S2 Agreement between the PMF predicted and observed PM_{2.5} in (a) summer and (b) autumn.

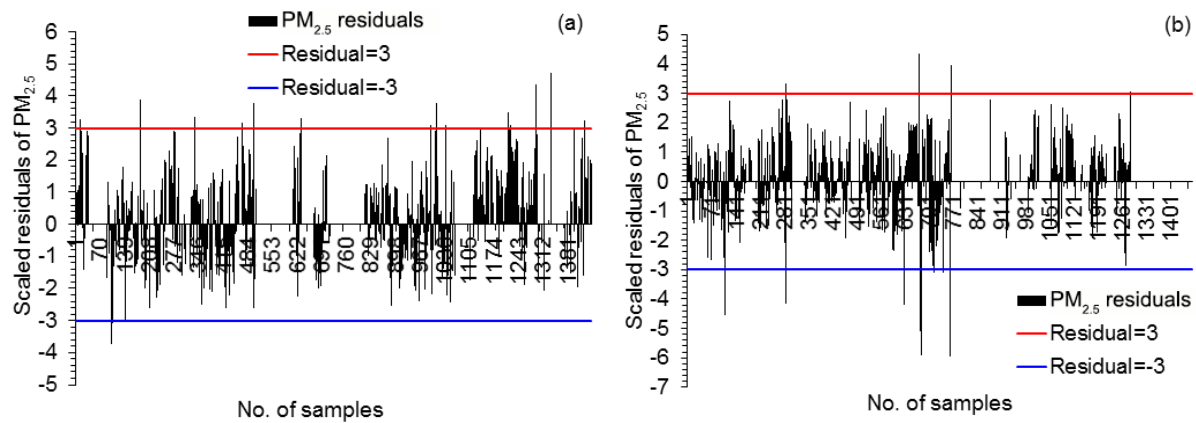
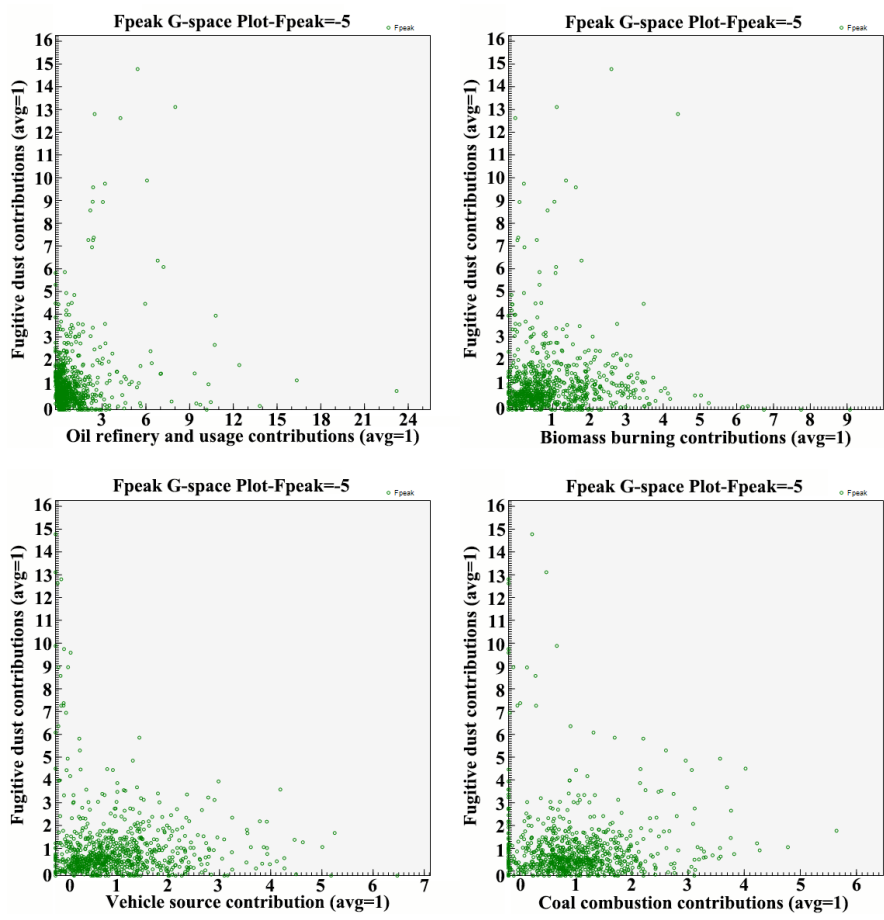


Figure S3 Scaled residuals for PM_{2.5} in (a) summer and (b) autumn.



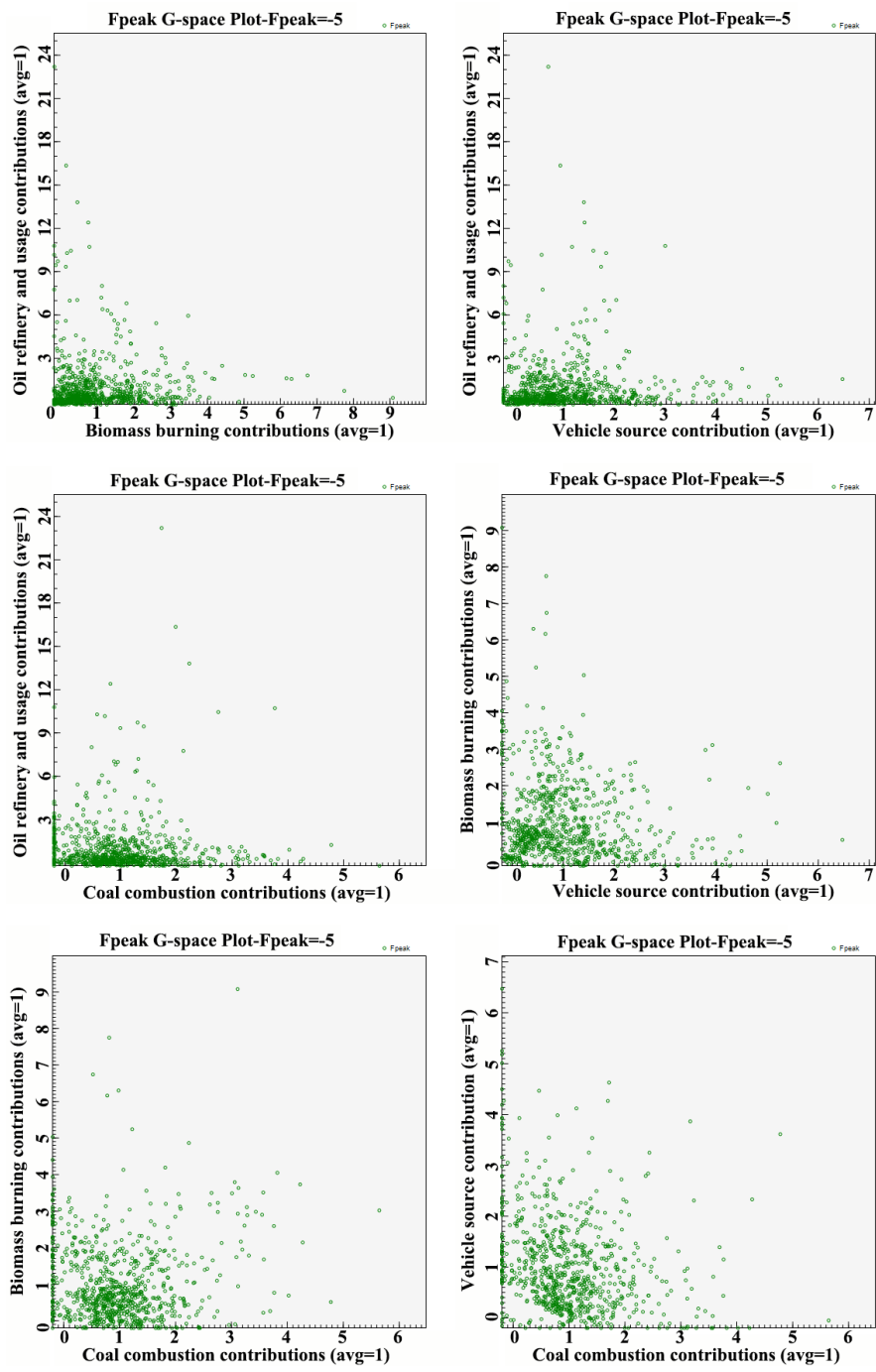
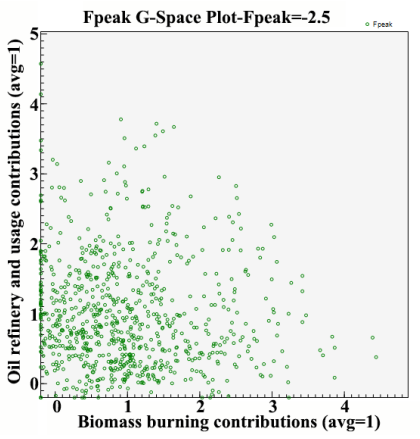
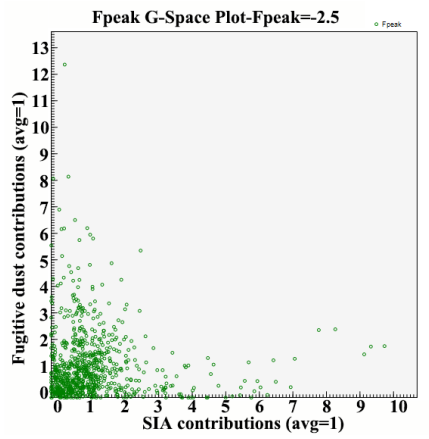
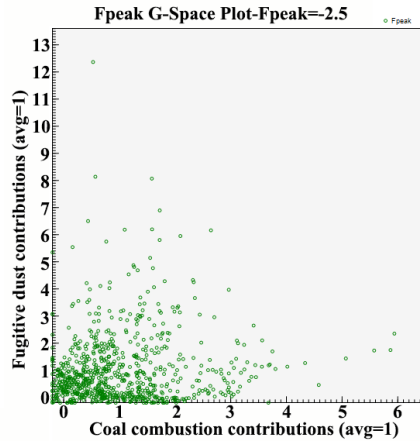
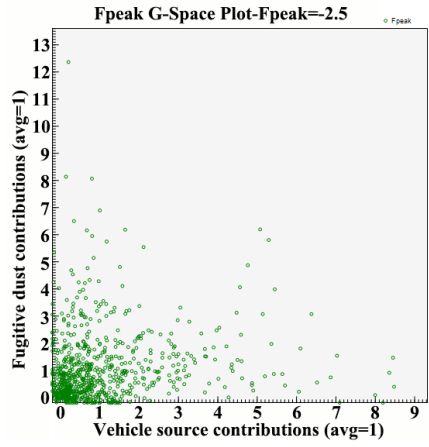
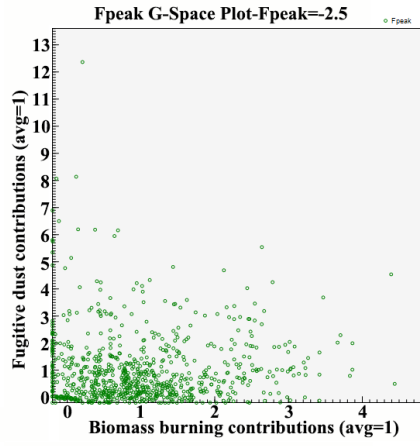
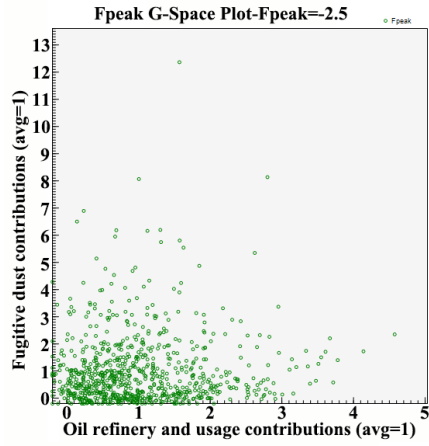
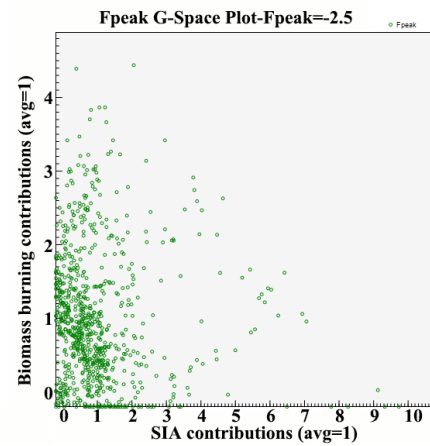
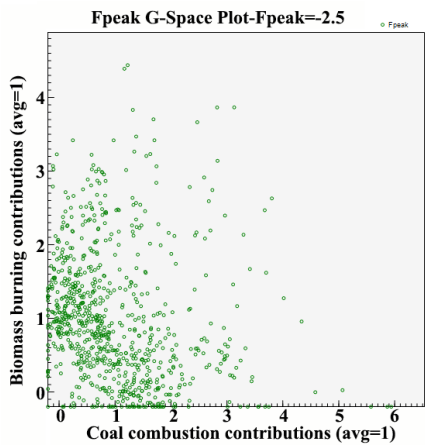
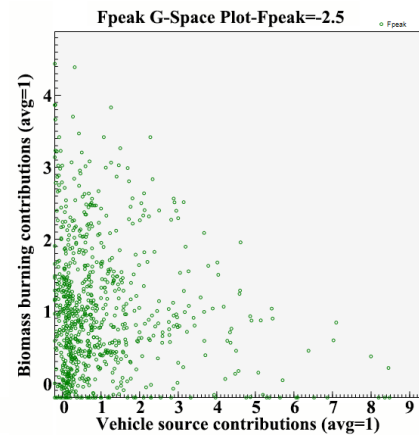
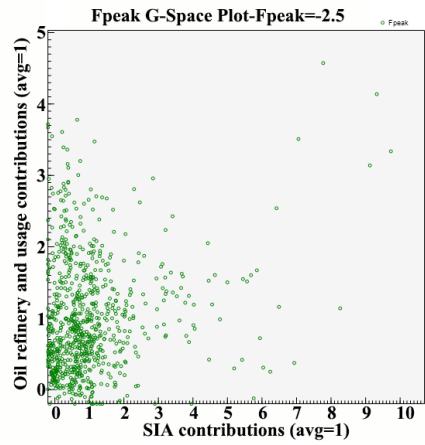
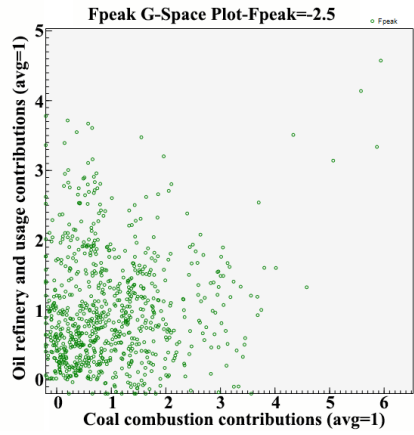
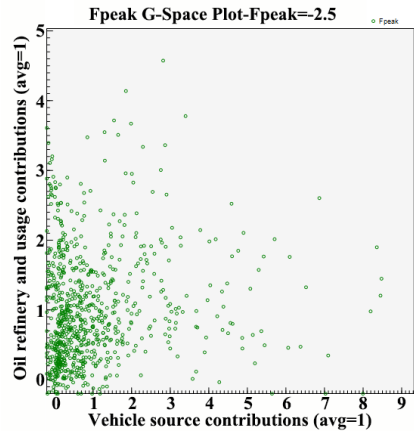


Figure S4 G-space plots with the rotational ambiguity controlled by FPEAK runs in summer.





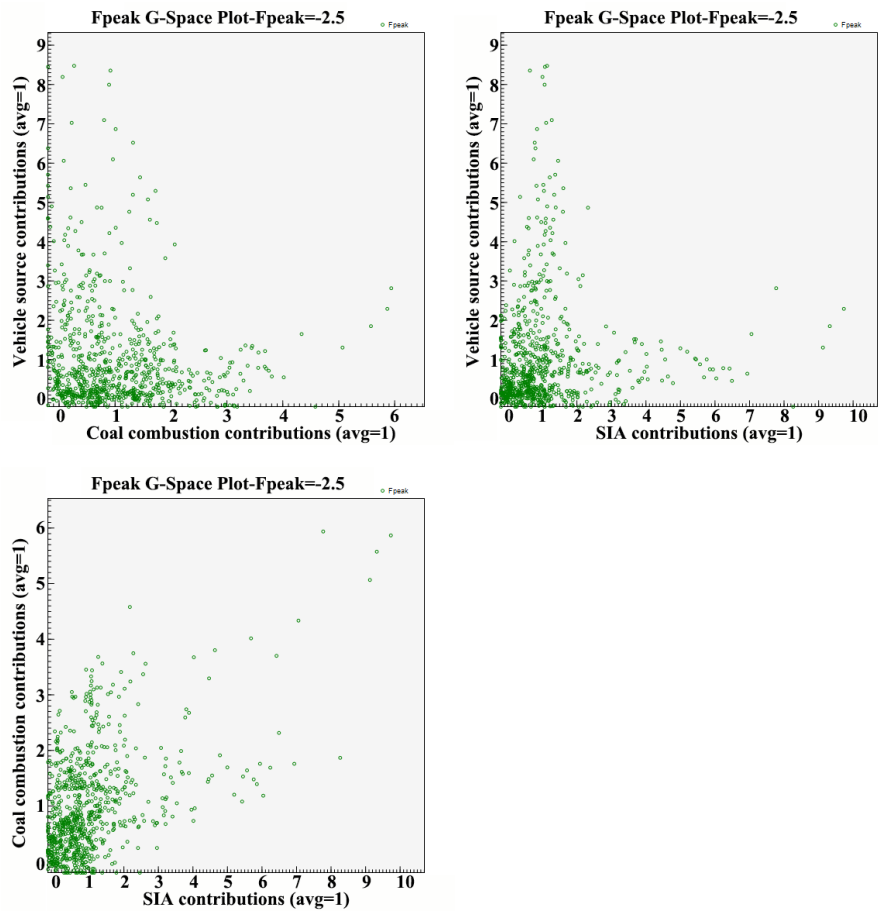


Figure S5 G-space plots with the rotational ambiguity controlled by FPEAK runs in autumn.

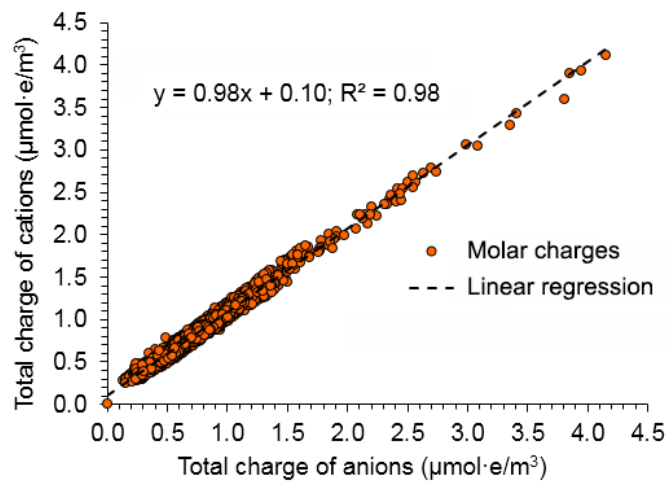


Figure S6 Relative abundances of molar charges of total cations and anions in $PM_{2.5}$ in autumn.

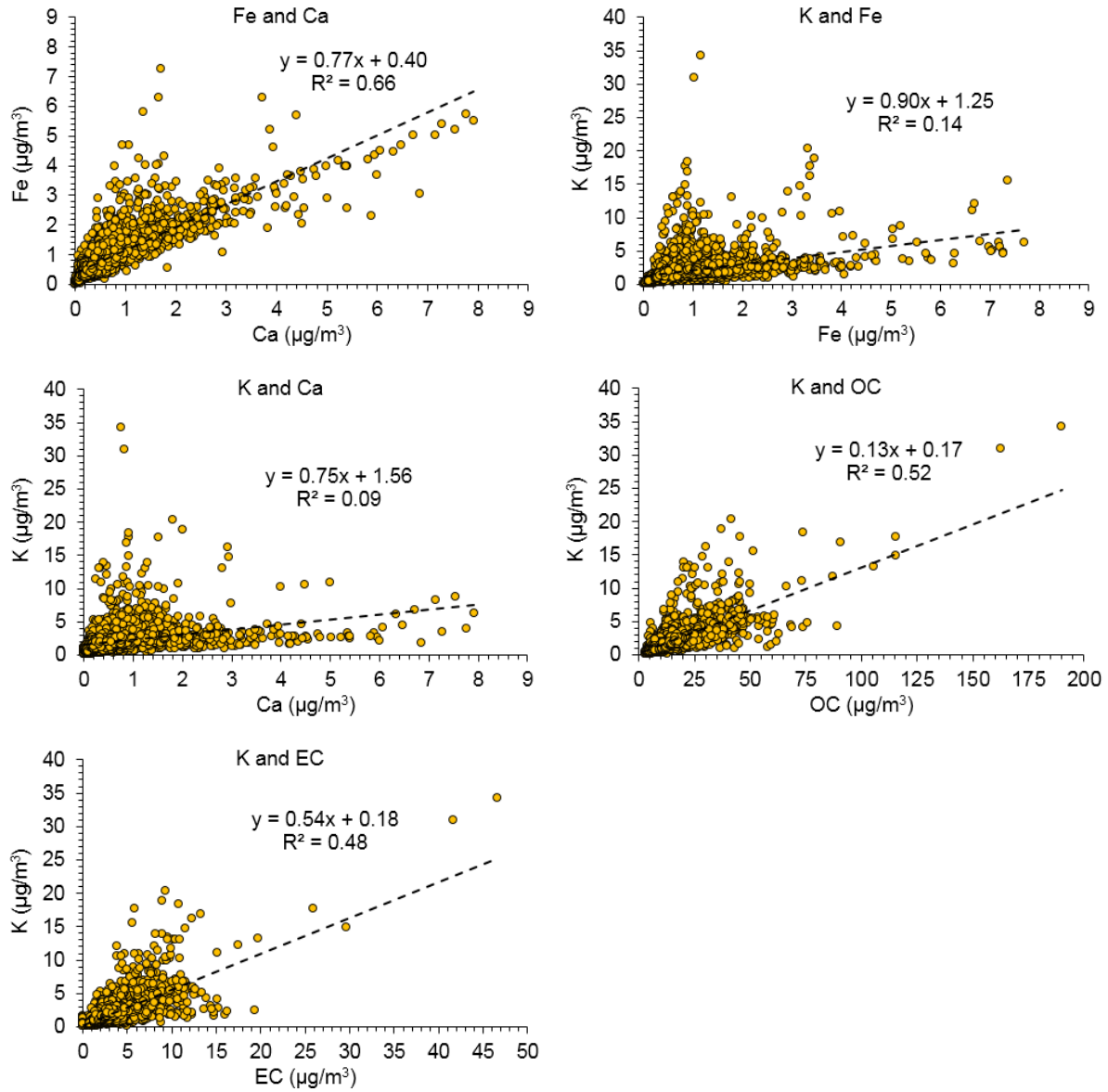


Figure S7 Correlations among OC, EC, K, Ca and Fe during the whole study period.

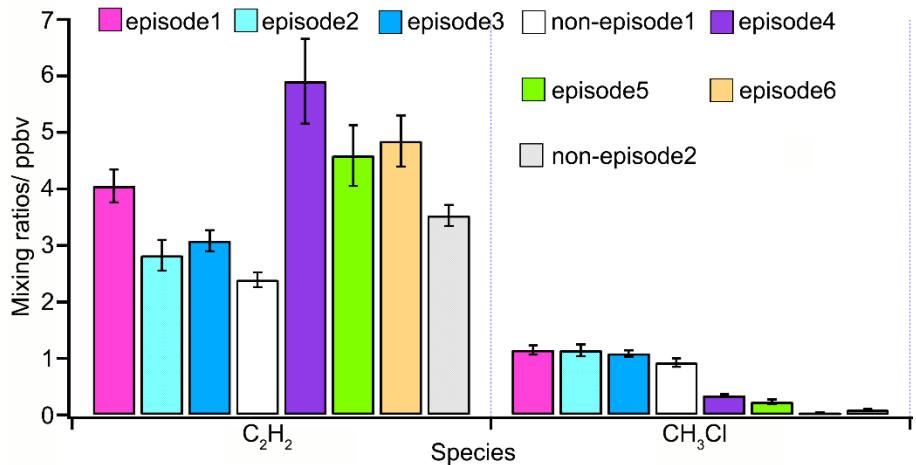


Figure S8 Mixing ratios of C_2H_2 and CH_3Cl in episodes and non-episodes.

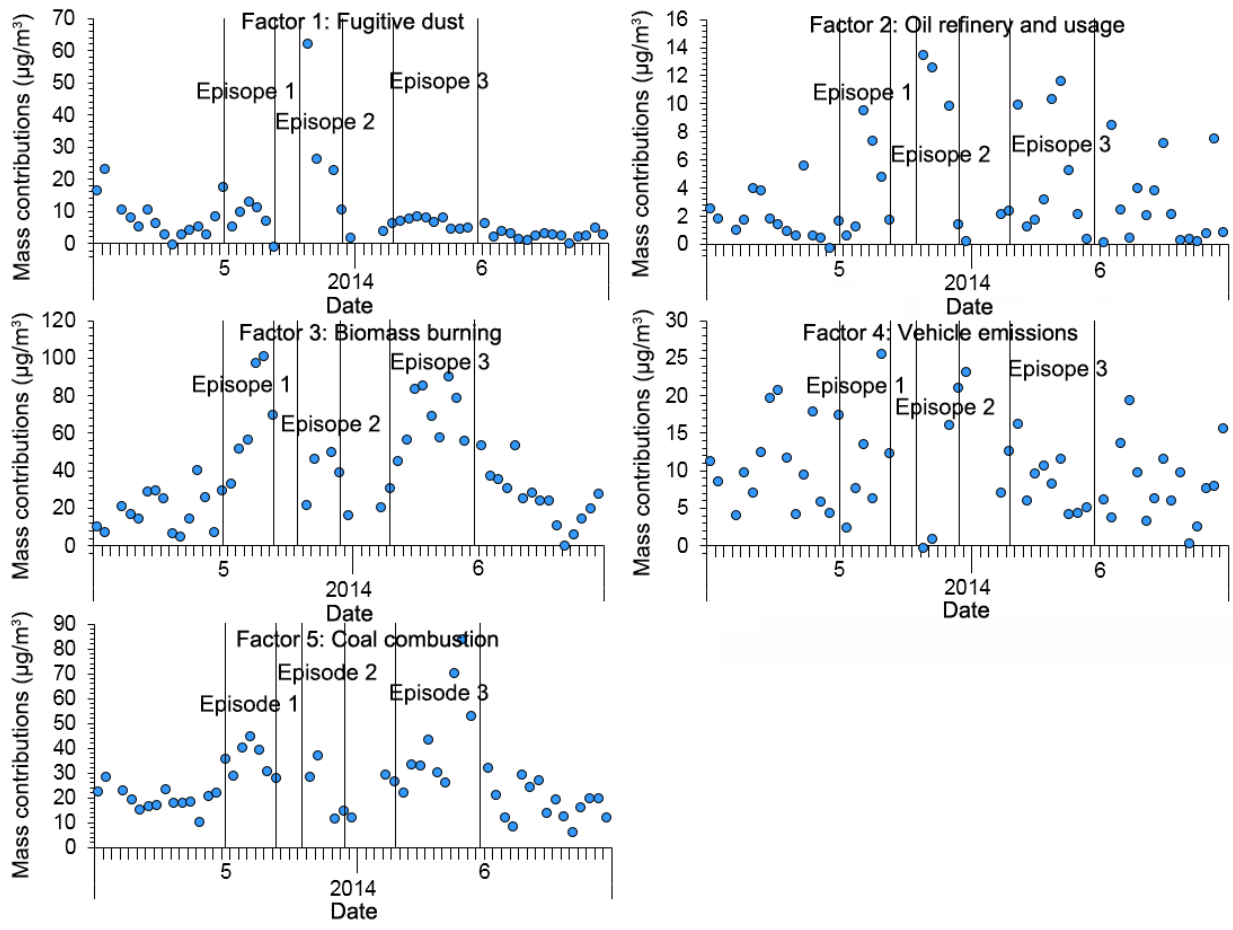


Figure S9 Day-to-day variations of source contributions to $PM_{2.5}$ in summer.

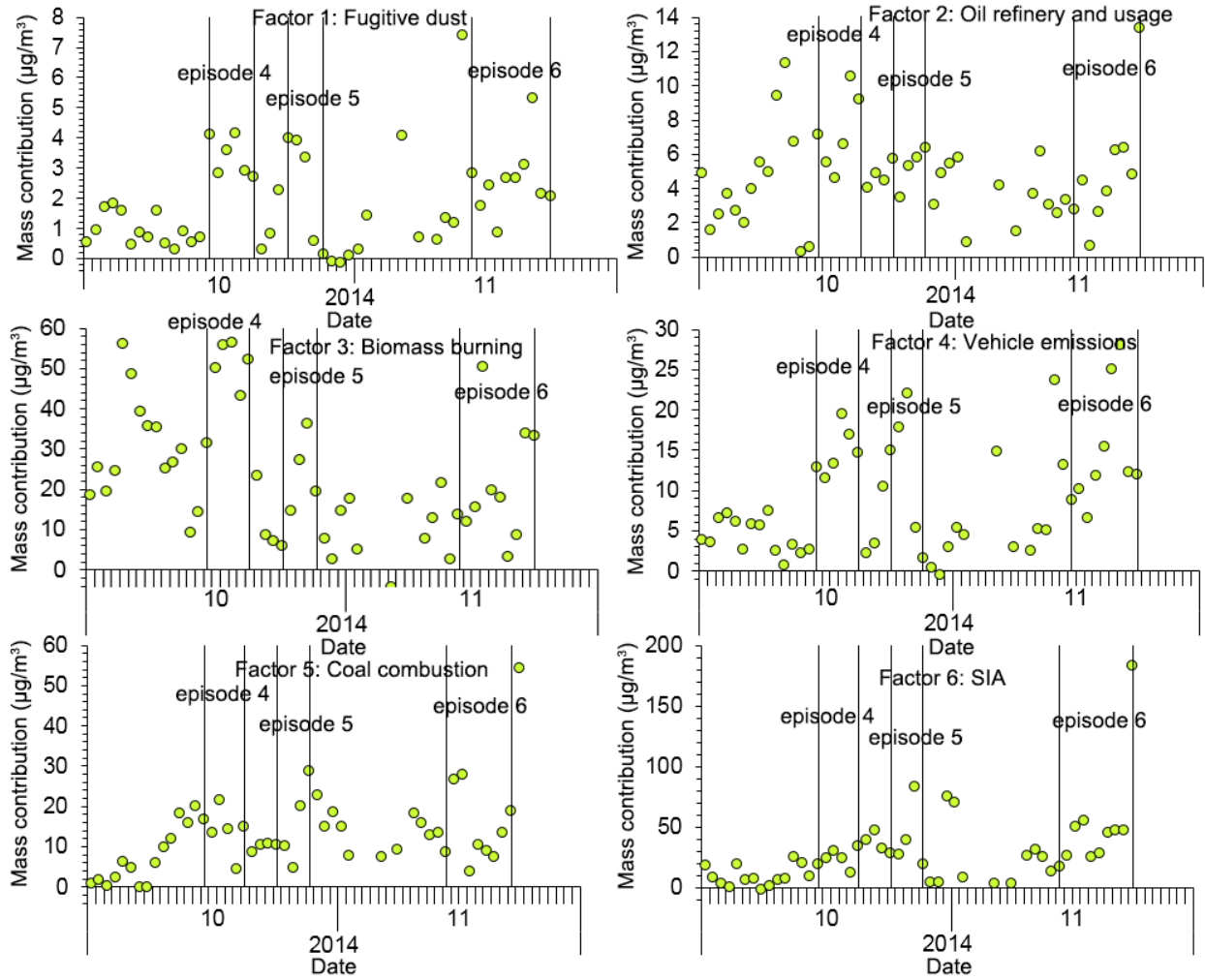


Figure S10 Day-to-day variations of source contributions to PM_{2.5} in autumn.

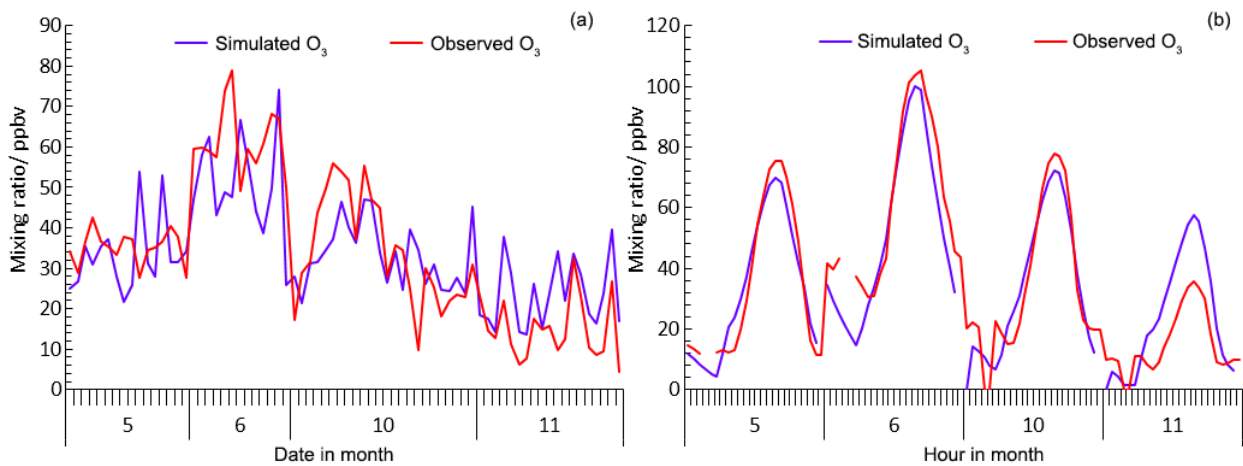


Figure S11 Agreements between the simulated and observed O₃ in (a) day-to-day variation and (b) diurnal pattern.

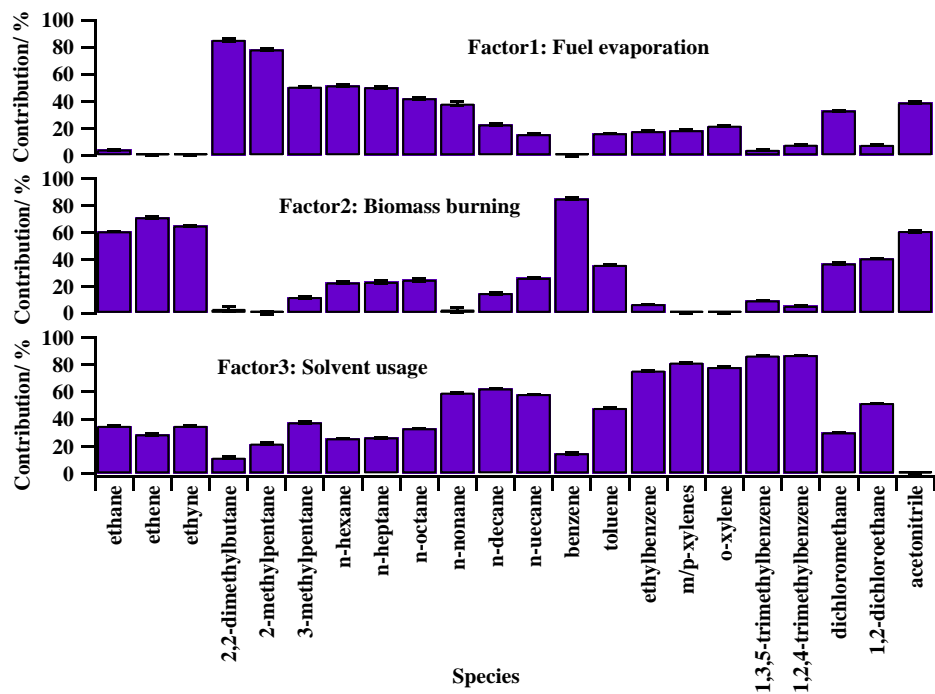


Figure S12 Source profiles of VOCs during PM_{2.5} episodes in autumn.

References:

Streets, D.G., Gupta, S., Waldhoff, S.T., Wang, M.Q., Bond, T.C., and Yiyun, B., 2001. Black carbon emissions in China. *Atmos. Environ.* 35, 4281-4296.